Materials Science and Engineering A 499 (2009) 337–341

Contents lists available at ScienceDirect

Materials Science and Engineering A

journal homepage: www.elsevier.com/locate/msea

Medium carbon steel deep drawing: A study on the evolution of mechanical properties, texture and simulations, from cold rolling to the end product

Ronald L. Plaut[a,*], Angelo F. Padilha[a], N.B. Lima[b], Clara Herrera[c], Antenor Ferreira Filho[d], Leandro H. Yoshimura[e]

[a] University of São Paulo, São Paulo, Brazil
[b] IPEN-CNEN/SP, São Paulo, Brazil
[c] Max-Planck-Institut für Eisenforschung, Germany
[d] Industrial Director, Brasmetal Waelzholz S/A, Diadema, Brazil
[e] CCS Consulting, São Paulo, Brazil

ARTICLE INFO

Article history:
Received 4 March 2007
Received in revised form 14 July 2007
Accepted 2 November 2007

Keywords:
Medium carbon steels
Texture
Mechanical properties
Deep drawing
Forming limit diagram
FEM simulations

ABSTRACT

Medium carbon steels are mostly used for simple applications; nevertheless new applications have been developed for which good sheet formability is required. This class of steels has an inherent low formability. A medium carbon hot rolled SAE 1050 steel has been selected for this study. It has been cold rolled with reductions in the 7–80% range. Samples have been used to assess the cold work hardening curve. For samples with a 50 and 80% thickness reduction, an annealing heat treatment has been performed to obtain recrystallization. The material has been characterized in the "as received", cold rolled and annealed conditions, using several methods: optical microscopy, X-ray diffraction (texture), Vickers hardness and tensile testing. The 50% cold rolled and recrystallized material has been further studied in terms of sheet metal formability and texture evolution during the actual stamping of a steel toecap that has been used to validate the finite element simulations.

1. Introduction

Carbon steels, particularly in the form of sheets are by far the most produced metallic materials worldwide. Despite that major part of its production is aimed at simple applications. Its processing technology and properties has been going through a continuous process of evolution and growth. The most significant segment, economically speaking, of the flat products may be linked to stampings, mainly the low-carbon, and mainly related to the automotive industry. These steels have a limited capability in terms of thermochemical treatments and, due to their low carbon content, cannot receive any further heat treatments. Hence, their mechanical properties are comparatively low, limiting their usage, requesting the application of medium and high carbon steels [1].

Nowadays, a great variety of new applications for medium and high carbon steels have been developed for which deep drawability is also requested. It is known that these steels present inherently a low workability and that forming conditions become more critical as carbon levels increase. For medium and high carbon steels, the pearlite lamellar morphology leads to low, undesirable mechanical properties during cold forming in high stress components, while a globular cementite improves toughness, cold formability and machinability [1,2].

Sheet metal formability depends mainly on anisotropy and, consequently, on texture. A BCC material has an ideal stamping texture when a large number of its grains is oriented with its {1 1 1} plane parallel to the sheet plane, known as the γ-fiber, ⟨1 1 1⟩//ND.

The texture of medium and high carbon steels in their different conditions, hot rolled, cold rolled or annealed, has seen little research work. Storojeva et al. [1] carried out work on the texture evolution and its microstructure on medium-carbon steels (0.36%C–0.53%Mn–0.22%Si) warm rolled. They concluded that texture does not change for different rolling and coiling temperatures, being characterized by the γ- and α-fiber, with a maximum in the {1 1 2}⟨1 1 0⟩ component. Walenteck et al. [2] studied the texture evolution in a high-carbon (0.79%C–0.9Mn–0.26%Si, wt.%) steel, after a 74% thickness reduction. They concluded that deformation texture obtained is typical of a cold-rolled BCC sheet, through the γ- and α-fiber, however with a weaker intensity when compared to low-carbon steels. The development of the deformation texture, both for low- and high-carbon content, is dependent on the differences in the initial texture and in the presence of a second phase,

* Corresponding author. Tel.: +55 11 3091 5637; fax: +55 11 3091 5243.
E-mail address: rlplaut@usp.br (R.L. Plaut).

0921-5093/$ – see front matter © 2008 Elsevier B.V. All rights reserved.
doi:10.1016/j.msea.2007.11.131

Table 1
Chemical composition (wt.%) of the SAE 1050 steel

C	0.472
S	0.0044
Mn	0.705
Si	0.1966
P	0.0155
Al	0.0361
Mo	0.001
N	0.025
Ni	0.0106
Cr	0.0212
Ti	0.0023
Nb	0.0011
V	0.0003
Cu	0.017
Pb	0.0003
Sn	0.0008
B	0.0002
W	0.0022

in the case cementite, in the high-carbon steels. Their deformation texture has been simulated for both steels and the results suggest that the interaction between grains has a larger influence on deformation texture than the effect caused by the actual presence of the second phase, i.e., the cementite lamellae.

The main objectives of this work are to study the texture, the mechanical properties of a medium-carbon steel during its processing stages, aiming at the understanding of its behavior during stamping. Performing the stamping simulation and comparing results with an actual piece, namely a steel toecap (ASTM Z41-1991 or EN 345 S1P), was the second objective.

2. Materials and methods

A hot-rolled medium-carbon steel SAE 1050 has been selected. Table 1 presents the chemical composition of the studied steel.

The steel has been cold rolled, with thickness reductions in the 7–80% range, in order to obtain the cold-work hardening curve. Rolling has been performed in an industrial reversible four-high rolling mill. The 50 and 80% cold-rolled samples (true strain $\varepsilon = 0.69$ and 1.6, respectively), were subsequently annealed at 700 °C, for 13 h in an industrial furnace containing 100% H_2, to obtain full recrystallization.

Materials characterization in the "as received", cold rolled and annealed conditions has been carried out using different techniques such as optical microscopy, X-ray diffraction (texture), Vickers hardness and tensile testing.

For the different processing stages X-ray diffraction has been used. Analysis has been conducted in a Rigaku horizontal texture goniometer (of the IPEN/CNEN-SP), with a Mo Kα1 ($\lambda = 0$ 7093 Å) radiation. For the orientation distribution function (ODF) evaluation, a specific program, developed at the same institution, has been employed. Analysis has been conducted at the rolled sample surface. Tensile testing has been carried out in a Zwick

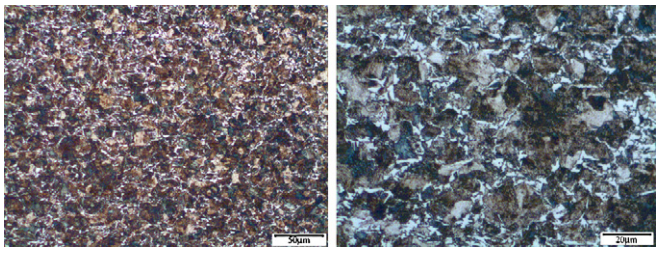

Fig. 1. Microstructure of the SAE 1050 steel—"as received" condition.

Table 2
Mechanical properties of the SAE 1050 steel in the "as received" condition

YS (N/mm^2)	665.33
TS (N/mm^2)	833.18
El 80 (%)	7.82
Hardness (HV)	226.7

YS = yield strength; TS = tensile strength; El (80) = elongation in 80 mm.

(model 1475) machine equipped with extensometer and hydraulic chucks, according to equivalent SAE standards (ABNT NBR 6673: 1980). From these tests the values of yield stress (YS), tensile strength (TS), total elongation, strain-hardening coefficient (n), normal anisotropy parameter (r_m) and planar anisotropy parameter (Δr) have been evaluated. These values have been used as inputs for the FEM sheet metal simulation program from AUTOFORM® [3].

3. Results and discussion

The SAE 1050 steel in the "as received" condition presented a pearlite–ferrite microstructure, as shown in Fig. 1. Table 2 shows the mechanical properties for the "as received" condition. Texture can be characterized by the strong {0 0 1} components, in the ⟨1 0 0⟩, ⟨2 1 0⟩ and ⟨1 $\bar{1}$ 0⟩ directions, TR = 4.1. The α- and γ-fiber are not present (Fig. 2). Strain hardening has been studied through Vickers hardness measurements in the section normal to the rolling direction. The SAE1050 steel showed a small hardening rate and, for reductions higher than 30%, there was a trend towards hardness saturation.

For larger cold reductions, the SAE 1050 steel presented low elongation, less than 2%, with a TS of the order of 1400 MPa. In the cold worked condition the steel has low ductility (i.e. takes high loads, however has little elongation), due to the ferrite–pearlite microstructure. The cementite hinders dislocation mobility, hence requiring higher loads to start moving them.

Figs. 3–5 show the ODF for the three cold reductions, namely 50, 70 and 80%. In general, the textures are typical of BCC cold-rolled materials. For 50% cold working, texture has completely changed with respect to the "as received" condition. The deformation texture is characterized by the fiber γ′, ⟨2 2 3⟩//ND, with the {2 2 3}⟨1 1 0⟩, {2 2 3}⟨4 7 2⟩ and {2 2 3}⟨1 4 2⟩ more intensive com-

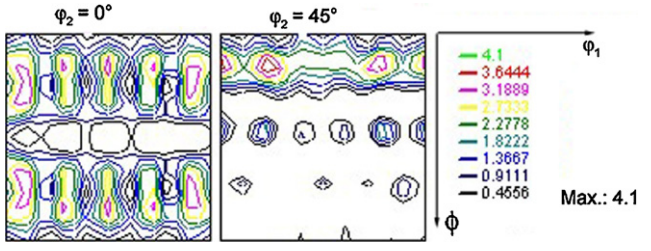

Fig. 2. ODF of the SAE 1050 steel in the "as received" condition.

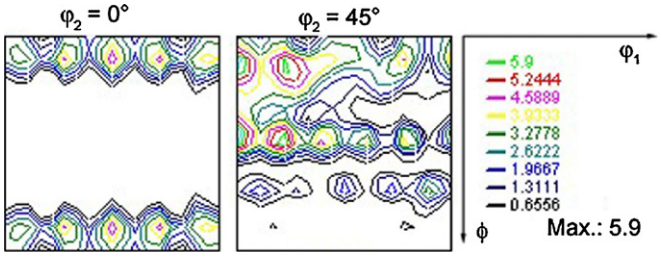

Fig. 3. ODF of the SAE 1050 steel with 50% cold working thickness reduction.

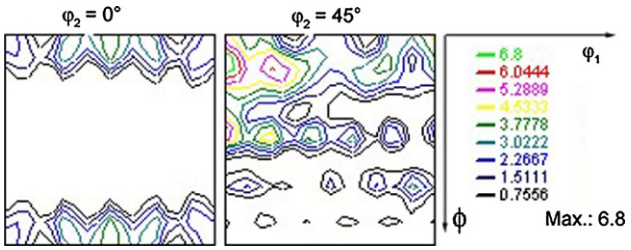

Fig. 4. ODF of the SAE 1050 steel with a cold working thickness reduction of 69%.

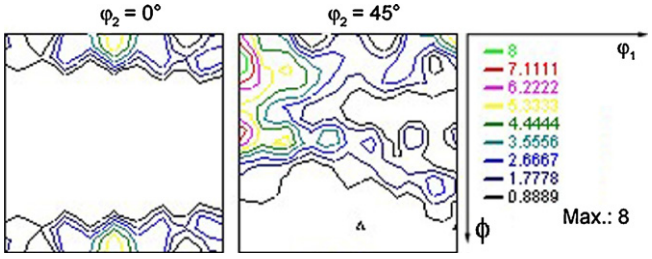

Fig. 5. ODF of the SAE 1050 steel with a cold working thickness reduction of 80%.

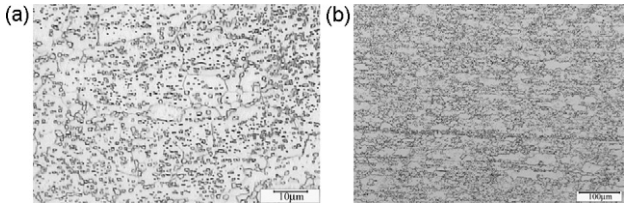

Fig. 6. SAE 1050 cold worked to (a) 50% and (b) 80% and recrystallized.

ponents, TR = 5.9, the ⟨1 0 0⟩//ND fiber, with the {0 0 1}⟨1 1 0⟩ and {0 0 1}⟨1 2 0⟩ components and the α-fiber, ⟨1 1 0⟩//RD was weak and heterogeneous. The γ′-fiber is typical for cold-worked low-carbon steels, being a variant of the γ-fiber, i.e., a rotation around the ⟨1 1 1⟩ axis [4,5].

Increasing thickness reduction to 70%, leads to a weakening of the ⟨1 0 0⟩//ND and γ′-fiber and the (0 0 1) [1 2 0], (0 0 1) [1 1 0] and (2 2 3) [1 $\bar{1}$ 0] are intensified, TR = 6.8. The two last ones are components of the α-fiber. With 80% thickness reduction, α-fiber continues to strengthen, with stronger {0 0 1}⟨1 1 0⟩ and {2 2 3}⟨1 1 0⟩ components, TR = 8. The γ-fiber that did not show up for smaller thickness reductions now starts to appear raging from (1 1 1) [1 $\bar{1}$ 0] down to (5 5 4) [2 2 $\bar{5}$] and with a decrease in the γ′-fiber intensity.

Fig. 6 shows the microstructure of the SAE 1050 steel cold worked with a thickness reduction of 50 and 80% in the annealed condition. It is characterized by its microstructure presenting a spherodized (or globulized) cementite within a ferritic matrix. Table 3 summarizes the mechanical properties of the SAE 1050 steel in the annealed condition, for both thickness reductions. Both yield stress (YS) and tensile strength (TS) presented a significant reduction after annealing, while elongation increased substantially

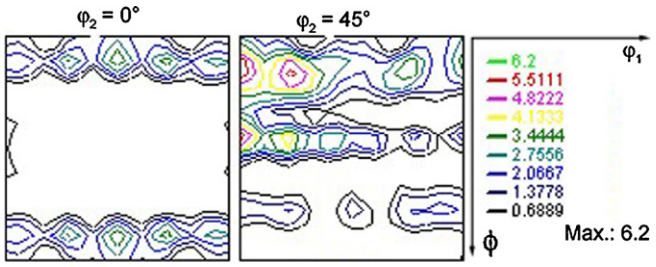

Fig. 7. ODF of the SAE 1050 steel with a thickness reduction of 50% and annealed.

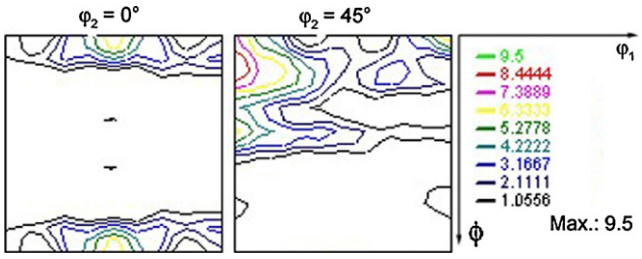

Fig. 8. ODF of the SAE 1050 steel with a thickness reduction of 80% and annealed.

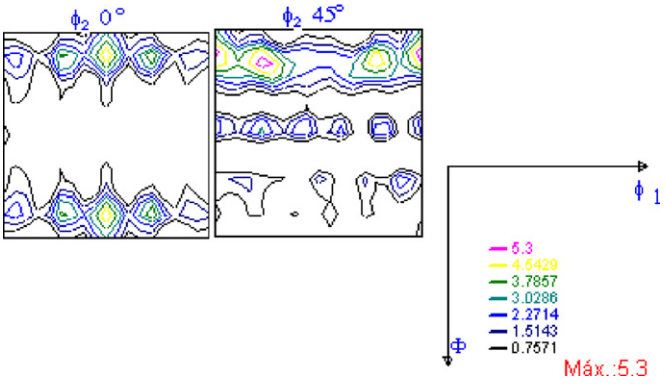

Fig. 9. ODF of the SAE steel with a thickness reduction of 50%, annealed and stamped, in a region close to the tip of the toecap.

in relation to the "as received" condition. In the 80% thickness reduction sample, YS, TS and Erichsen index (E.I.) are lower, while elongation, for an annealed 50% thickness reduction, it is higher. Although the r_m has increased with thickness reduction, the corresponding value for Δr is high, leading towards a decrease in deep-drawability, since the main goal is to maximize r_m and to minimize Δr (Δr=0).

Figs. 7 and 8 present the ODFs of the SAE 1050 steel in the recrystallized condition, after a thickness reduction of 50 and 80%, respectively. The 50% cold worked and annealed material presented the (0 0 1) [1 $\bar{1}$ 0] and (2 2 3) [1 $\bar{1}$ 0] components with greater intensity, TR = 6.2. This last component belongs to the γ′-fiber, ⟨2 2 3⟩//ND, having smaller intensity, similar to the α-partial fiber, ⟨0 1 1⟩//RD. The 80% cold rolled and annealed steel presented an α-fiber with the (2 2 3) [1 $\bar{1}$ 0] components and one (0 0 1) [1 $\bar{1}$ 0] with

Table 3
Mechanical properties of the SAE 1050 steel, cold worked and annealed

% Def.	YS (N/mm²)	TS (N/mm²)	El 80 (%)	n	r_m	Δr	Hardness (HV)	E.I. (mm)
50	333.44	490.69	24.41	0.19	0.85	0.22	143.6	11.83
80	303.61	470.52	28.59	0.18	1.07	−1.28	142.2	9.0

YS = yield strength; TS = tensile strength; El (80) = elongation on 80 mm; n = hardening exponent; r_m = normal anisotropy index; Δr = planar anisotropy index and E.I. = Erichsen index.

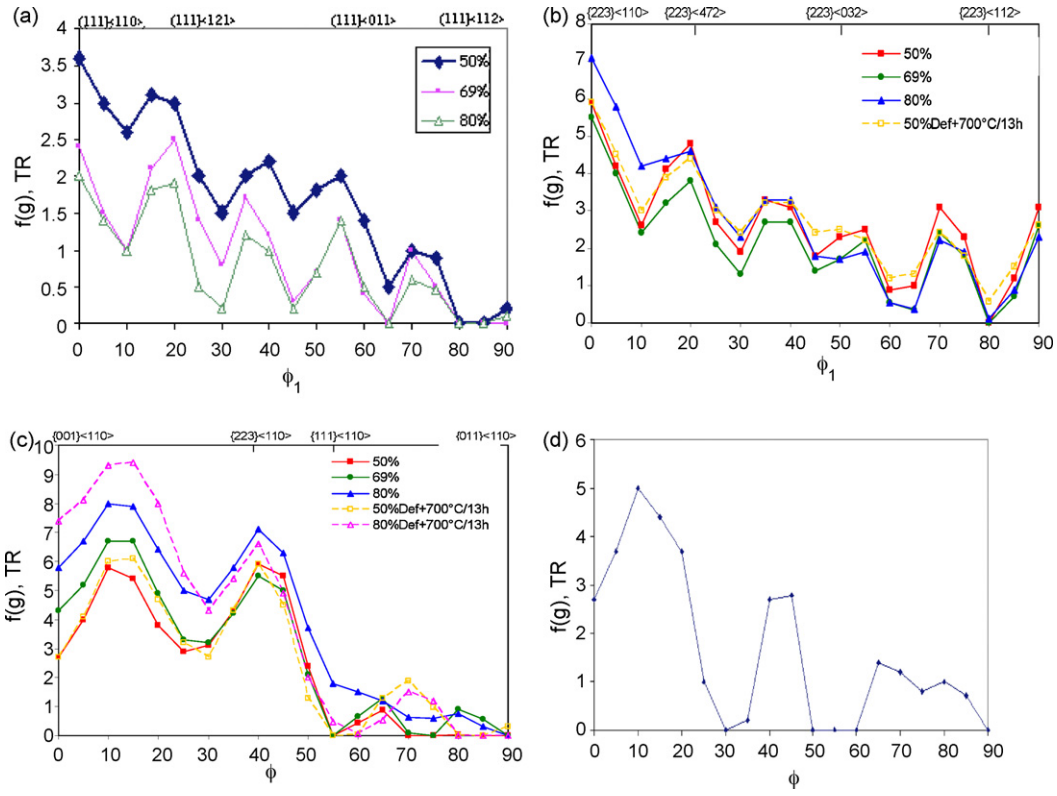

Fig. 10. Evolution of the (a) γ-fiber, (b) γ′-fiber, (c) α-fiber for the SAE 1050 steel, for different thickness reductions and annealed and (d) for the tip of the stamped toecap.

greater intensity, TR = 9.5. The γ-fiber did not show up in any of the samples. For the 50% cold worked and annealed SAE 1050 steel, the hardening curve followed closely the Hollomon-type relationship given by $\sigma\,(\mathrm{N/mm^2}) = 841\varepsilon^{0.19}$.

Fig. 9 shows the ODF for the SAE 1050 steel that has been industrially cold rolled with a 50% thickness reduction, annealed and taken for a stamping operation, specifically, for the production of steel toe caps (see Fig. 11). In the region close to the toetip, it may be observed that no major texture evolution occurred (comparing Figs. 7 and 9).

Fig. 10 presents the summary of the texture evolution for the studied steel in the various stages: cold worked and annealed, in

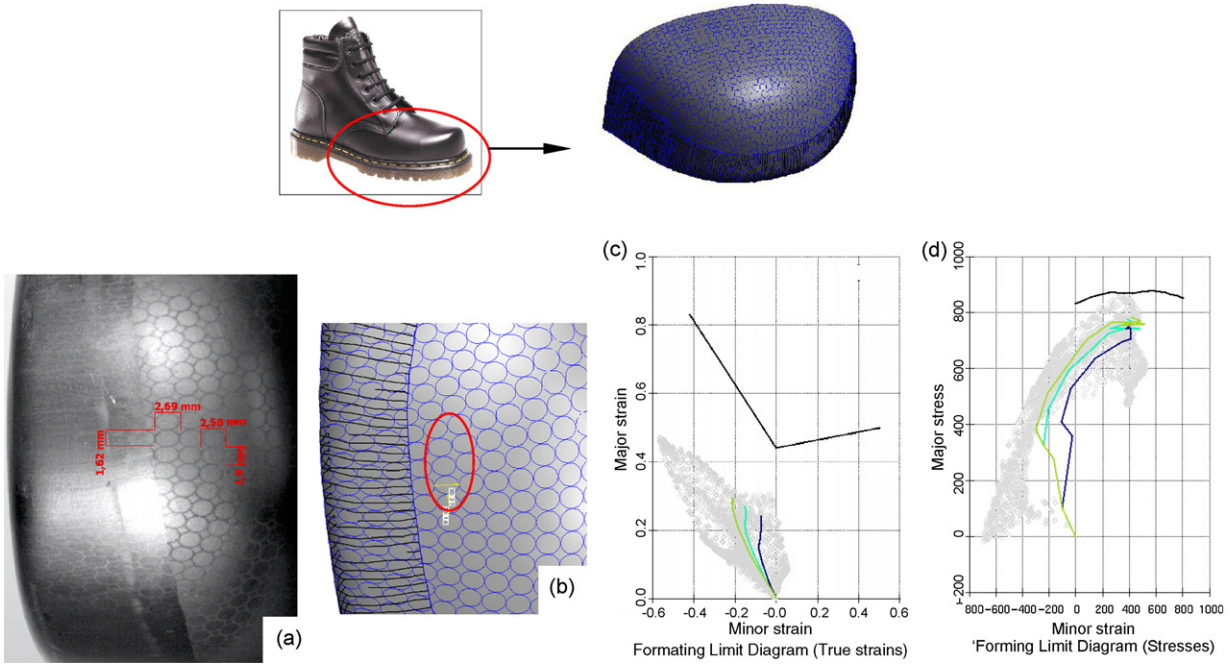

Fig. 11. Upper: safety-boot and steel toecap. Lower: (a) actual readings taken at the steel toecap tip; (b) simulation of the same region; (c) FLD for strains and (d) FLSD showing stress path evolution. Path on figures are those associated with the region containing the tip of the toecap.

the form of the γ-, γ′-, and α-fiber, present in the steel. It may be observed from Fig. 10a that the γ-fiber has been strengthened with the increase in thickness reduction, despite its intensity not being very high when compared to the α-fiber. If this result is compared to the results of a high carbon steel [2], it could be observed that despite the γ-fiber being more homogeneous in the high carbon steel, its intensity is small, close to 5. Hence, in rolling of a steel with a second phase, textures are not very strong. After annealing the γ-fiber vanished completely. The γ′-fiber (Fig. 10b) did not present any significant variation for the smaller thickness reductions, while for larger reductions in thickness, say 80%, its intensity drops. On annealing, the γ′-fiber for the 50% thickness reduction, did not present significant changes, while for 80% reduction that fiber vanished. The α-fiber (Fig. 10c) became more intense with the increase in thickness reduction, the $\{2\,2\,3\}\langle 1\,1\,0\rangle$ and a close to $\{0\,0\,1\}\langle 1\,1\,0\rangle$ components are the strongest. The $\{1\,1\,1\}\langle 1\,1\,0\rangle$ component that did not appear for lighter reductions, just showed up after a 80% thickness reduction. The α-fiber, in the 50% cold worked and annealed, presented little difference in relation to the cold worked steel. In the 80% cold worked and annealed steel, the α-fiber presented some strength increase along the $\{0\,0\,1\}$ and $\{1\,1\,2\}$ planes. Annealing the SAE 1050 steel after various thickness reductions does not change significantly the deformation texture. For stronger reductions, annealing texture presents an increase in the α-fiber, while the γ- and γ′-fiber vanished. A 50% reduction produces the best drawing texture, because the γ′-fiber is close to the γ-fiber. Fig. 10d also indicates that there was no major change in the α-fiber of the stamped toecap (comparing Fig. 10c and d).

4. Finite element simulation

Actual stampings have been carried out using the above mentioned SAE 1050, cold rolled 50% and annealed sheets, under industrial production conditions, aiming at the production of the steel toe caps, used in the manufacture of safety boots (see item 1 above). Starting thickness was 1.7 mm and the material characteristics were given by $K = 841$ MPa, $n = 0.19$, $R_0 = 0.88$, $R_{45} = 0.74$, $R_{90} = 1.03$ and $\mu = 0.2$. As an initial evaluation of the FLD, the NADDRG [6] empirical equation has been used, providing a rough estimate of the FLDo = 43%. For the study of this stamping a up-to-date comprehensive software AUTOFORM® (Ver. 4.07) has been used, in order to analyze thickness variations, distribution of strains and stresses, mainly at the steel toe boot tip. Fig. 11a presents the actual stamping with circle engravings used to measure real strains. Fig. 11b presents the simulation for the same area of interest, i.e., the tip of the toecap. The actual strain path in that region can be followed by the tracings in Fig. 11c and the actual stress path given by the tracings in Fig. 11d. Experimental and calculated strain values are in good agreement.

5. Conclusions

(i) The SAE 1050 steel in the as-received conditions presented a pearlite–ferrite microstructure, with a weak texture, wherein the α- and γ-fiber were not present.
(ii) Strain hardening of the SAE 1050 steel was small. For large thickness reductions, elongations were very low, smaller than 2% and a YS close to the TS of about 1400 MPa. Associated textures were typical of those found in BCC cold-rolled materials.
(iii) Texture after annealing and recrystallization did not suffer any significant changes in relation to the deformation texture. For larger thickness reductions, annealing texture increased the α-fiber, while the γ- and γ′-fiber vanished. A thickness reduction close to 50% before annealing leads to the best deep-drawing texture, since the γ′-fiber is close to the γ-fiber. On annealing, the YS and the TS decrease, while elongation increases with the increase in prior deformation. The values of r_m and Δr increased with rolling reduction.
(iv) On stamping a 50% thickness reduction and annealed SAE 1050 steel, observing a typical component such as the toecap tip, there was no major texture change.
(v) The simulation of a component showed that it produced reliable results indicating that the SAE 1050, 50% cold reduced and annealed steel, produces adequate simulations, even for these higher-than-the-usual carbon steels.

Acknowledgements

The authors would like to thank Brasmetal Waelzholz for its support during the experiments and production of samples and also the CNPQ for the financial support of a pos-doctoral industrial fellowship (process no. 308839/2005-6).

References

[1] L. Storojeva, D. Ponge, R. Kaspar, D. Raabe, Acta Mater. 25 (2004) 2209–2220.
[2] A. Walenteck, X. Hu, M. Seefeldt, P. Van Houtte, Mater. Sci. Forum 495–497 (2005) 369–374.
[3] AutoForm Engineering GmbH, Zürich, Switzerland.
[4] H. Inagaki, ISIJ Int. 34 (1994) 313–321.
[5] D. Daniel, J. Savoie, J.J. Jonas, Acta Metall. Mater. 41 (1993) 1907–1920.
[6] D. Banabik, H.-J. Bunge, K. Pöhlandt, A.E. Tekkaya, Formability of Metallic Materials, Springer, Berlin, 2000.